$\delta^{34}S$ variations in pyrite: An experimental study of sulfate reduction to evaluate the unusual S-isotope signature in Archean Pyrite

Liz Peters

Advisors:

Dr. James Farquhar

James Dottin III

GEOL 394

30 April 2018

Table of Contents

Symbols to Reference

Symbol	Physical meaning
SRB	Sulfate reducing bacteria
Ga	Billion years old
^{33}S, ^{34}S, and ^{36}S	Minor sulfur isotopes
O_2	Oxygen
CO_2	Carbon dioxide
DIC	Metabolize dissolved inorganic carbon
H^+	Hydrogen
S°	Elemental sulfur
Fe^{2+}	Ferrous (Iron II)
^{33}S	Sulfur thirty-three
UV	Ultra-violet
$\delta^{33}S$	Delta thirty-three sulfur
$\delta^{36}S$	Delta thirty-six sulfur
$\Delta^{33}S$	Cap delta thirty-three sulfur
$\Delta^{36}S$	Cap delta thirty-six sulfur
SO_4^{2-}	Sulfate
S^{2-}	Sulfide
Fe_3S_4	Greigite
S_xS^{2-}	Polysulfide
HS^-	Hydrogen sulfide
FeS_2	Pyrite
HRM2	*Desulfobacterium autotrophicum* HRM2
$FeCl_2$	Ferrous chloride
nm	Nanometers
H_2S, HS^-, S^2	Forms of dissolved hydrogen sulfide
$BaCl_2$	Barium chloride
$BaSO_4$	Barium sulfate
$CHCl_3$	Chloroform
MeOH	Methanol
Ag_2S	Silver sulfide
EPMA	Electron Probe Microanalyzer
AIMLab	Advanced Imaging and Microscopy Laboratory
EDS	Energy-dispersive spectrometry
BSE	Backscattered electron
SF_6	Sulfur hexafluoride
ATCC	American Type Culture Collection
N_2	Nitrogen in gas state
‰	Per mille
MSR	microbial sulfate reduction

Abstract

Prior studies of sulfur isotopes of pyrite from Archean rocks reveal anomalies that have both positive and negative capital delta sulfur thirty-three ($\Delta^{33}S$) compositions. The general understanding is that atmospheric elemental sulfur (S°) contributes positive $\Delta^{33}S$ compositions in Archean rocks with pyrite and atmospheric sulfate (SO_4^{2-}) contributes the negative $\Delta^{33}S$. The positive and negative $\Delta^{33}S$ compositions of pyrite implies sourcing of sulfur from both species. Although both sources play an important role in contributing to the S-isotope heterogeneity, the pathways for incorporation and preference of S° verse SO_4^{2-} in pyrite are not fully understood.

Archean pyrite is a direct product of sulfate reduction. Assuming the $\Delta^{33}S$ of SO_4^{2-} is preserved during reduction, it is expected that the pyrite shows a negative $\Delta^{33}S$ composition. This is, however, not observed, and has led to questions related to the processes in the atmosphere and oceans that lead to a varying $\Delta^{33}S$ signal. Sulfide is produced by sulfate reducing bacteria (SRB) that reduced SO_4^{2-}. In the Archean, this sulfide might then form iron sulfide after exchanging isotopes and or reacting with S° having a positive $\Delta^{33}S$. One hypothesis is that S° does an exchange reaction free sulfide formed from microbial sulfate reduction (MSR). This sulfide then reacts with Fe^{2+} to form pyrite with variable $\Delta^{33}S$.

Here this thesis tests these hypotheses with low-temperature pyrite formation experiments. The results from experiments indicate that pyrite can be formed from the reduction of sulfate to sulfide in ferrous iron bearing solutions (Fe^{2+}). and, furthermore, that a greater abundance of pyrite formed when elemental S was present, and that this pyrite acquired an isotopic composition that was influenced by the isotopic composition of S°. The sulfur isotopic compositions of elemental sulfur, sulfate, and pyrite in the experiments are consistent with a role of elemental sulfur in pyrite formation.

Starting late August until mid-May low-temperature experiments were conducted, a total of three separate sets of experiments underwent a series of methods to test sulfide production, sulfate fractionation, and S° exchange. Twelve experiments were started in mid-December 2017, using sulfate with a $\Delta^{33}S$ label to trace sulfur derived from sulfate reduction, and to more precisely define the role of sulfate and elemental sulfur in pyrite formation of these experiments. The cultures have been tested with Cline reagent to evaluate free sulfide.

The experiments were performed in triplicate.

- The first group was the control group and utilized a solution used to verify the chemistry was correct. The solution, contained various salts including sodium sulfate, ferrous iron, and elemental sulfur, no bacteria added.
- The second group of experiments was designed to test what forms with a salt solution, containing elemental sulfur, and sulfate-reducing bacteria, in the absence of ferrous iron.
- The third group of experiments was designed to test what kind of isotopic signatures come from just the salt solution, ferrous iron, and sulfate-reducing bacteria, without elemental sulfur.

- The fourth group of experiments was designed to test the iron sulfur mineral that forms from the salt solution, ferrous iron, elemental sulfur, and sulfate-reducing bacteria.

Refer to table 1 for sample group numbers and the components in them. For these twelve experiments it was decided to increase the number of moles of ferrous iron to be sure that there was excess ferrous iron relative to sulfur. Additionally, by increasing the number of cultures to twelve instead of four, it was decided to decrease the amount of salt solution from 100 mL to 50 mL and decrease the moles elemental sulfur accordingly to the necessary amount of moles needed in the salt solution.

Table #1, Triplicate Experiments

Label	Sample # and contents in sample	Left out
Group #1	Fe^{2+}, S°, and aqueous SO_4^{2-} (with $\Delta^{33}S$ label) salt solution	Bacteria
Group #2	S°, bacteria, and aqueous SO_4^{2-}(with $\Delta^{33}S$ label) salt solution	Fe^{2+}
Group #3	Fe^{2+}, bacteria, and aqueous SO_4^{2-} (with $\Delta^{33}S$ label) salt solution	S°
Group #4	Fe^{2+}, S°, bacteria, and aqueous SO_4^{2-} (with $\Delta^{33}S$ label) salt solution	

Background

Microbial sulfate reduction is a global process that takes place preferentially in coastal marine environments. Figure 1 (Bowles et al., 2014) shows the global estimates of marine microbial reduction rates. From this figure, it is evident that sulfate reduction is widespread and that reduction rates increase along continental shelves and coastal margins relative to the middle of the oceans. Considering sulfate salts are soluble in water and have high concentrations in ocean water, making dissolved sulfate higher than molecular oxygen in sediments, microbial sulfate reduction becomes the most important mineralization pathway for organic matter in marine sediments and also controls oxygen levels (Rickard, 2014).

From a geological perspective, the earliest known evidence for SRB is preserved in the S-isotope composition of sedimentary rocks that date back to 3.49 billion years old (Ga) (Buick and Dunlop, 1990 Shen et al 2010, Ueno et al., 2009). Generally, the process

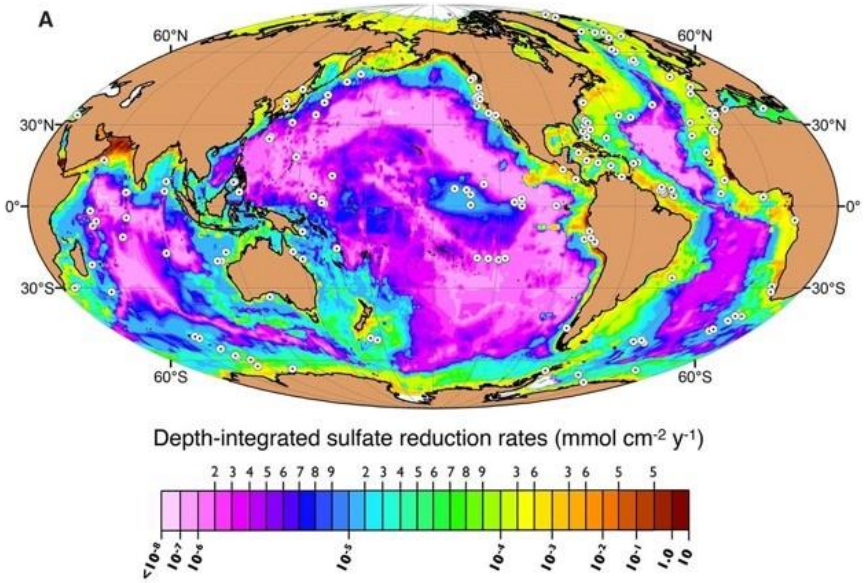

Figure 1. Map of the global effect of microbial reduction (from Bowles et al., 2014)

of sulfate reduction through SRB produces depletions in the minor sulfur isotopes (^{33}S, ^{34}S, and ^{36}S) relative to major isotope ^{32}S (Shen et al. 2009). The geologic time of the Archean Eon is of particular interest, as early studies by Canfield (2001) have shown specific fractionation signals when SRB appeared on Earth.

The chemical composition of oceans and the atmosphere during the Archean was different than that observed today, and its understanding is essential in evaluating S-isotope variations as a result of sulfate reduction. The Archean ocean is suggested to have been 30–40°C warmer than the ocean today (Ohmoto, 1992). In addition, Archean oceans had a pH of ~6.5 to 7.0 so it is slightly more acidic, than modern ocean water (Halevy and Bachan, 2017). The Archean atmosphere was different as there was no free oxygen (O_2) and the partial pressures of CO_2 was higher (Kasting, 1993). So, the bacteria had to be able to metabolize dissolved inorganic carbon (DIC), and use hydrogen (H^+) ions, as

an electron donor for growth. In the Archean, sulfate reducing bacteria (SRB) would have lived in the presence of elemental sulfur (S°) and ferrous (iron II, Fe^{2+}) in solution. Understanding the significance of the roles played between bacteria, sulfur, and iron species in the Archean eon, may lead to finding out how exobiology exists on other planets.

Motivation

To understand the Archean environment and the Earth during the Archean Era, fractionation of isotopes of oxygen, nitrogen, carbon, and sulfur have been studied and used to identify the processes leading to observed isotopic variability. Farquhar et al. (2001), determined that in the Archean there was mass-independent fractionation of sulfur thirty-three (^{33}S) fractionation due to the lack of ozone reflecting an increased interaction with ultra-violet (UV) radiation. Mass-independent fractionations are described by variations in capital delta notation ($\Delta^{33}S$ and $\Delta^{36}S$), where

$$\Delta^{33}S = \delta^{33}S - [\left(\frac{\delta^{34}S}{1000} + 1\right))^{0.515}] \times 1000. \text{ and}$$

$$\Delta^{36}S = \delta^{36}S - [\left(\frac{\delta^{34}S}{1000} + 1\right))^{1.90}] \times 1000.$$

These equations describe the excess or deficiency of ^{33}S or ^{36}S relative to a reference "mass-dependent" fractionation arrays which are given by $\delta^{33}S \approx 0.515\ \delta^{33}S$ and $\delta^{36}S \approx 1.9\ \delta^{33}S$.

The $\Delta^{33}S$ signals for sedimentary rocks are near zero for the Proterozoic Eon and Phanerozoic Eon; however, the signals for the Archean show positive and negative values for $\Delta^{33}S$. This anomaly is shown and described in the plot below (Fig 2: Farquhar, 2007). Pyrite formation is initiated by reaction of ferrous iron with sulfide that comes from reduction of sulfate (SO_4^{2-}) by microbial sulfate reducers (Berner, 1970; Rickard 2014). Sulfate in the Archean is thought to have negative $\Delta^{33}S$ (Farquhar et al., 2000; Farquhar and Wing, 2004); so, a negative $\Delta^{33}S$ was expected for pyrite from sulfate reduction. However, a lot of the data presented in Figure 2 is for pyrite and much of the data has positive $\Delta^{33}S$. It has been proposed by several authors that the pyrite that formed in the Archean was receiving more sulfur directly from S° instead of SO_4^{2-}.

Luther (1991), proposed that elemental sulfur and polysulfide can contribute directly to the formation of pyrite by:

1.) $Fe^{2+} + S^{2-} \rightarrow FeS \xrightarrow{S^8} Fe_3S_4 \xrightarrow{S^8} FeS_2$.

For this reaction, the Fe^{2+} reacts with sulfide (S^{2-}) to produce an iron sulfide, then directly reacts with S° to produce greigite (Fe_3S_4), then reacts again with the S° to produce pyrite. The second reaction is:

2.) $Fe^{2+} + S_5S^{2-} + HS^- \rightarrow FeS_2 + S_4S^{2-} + H^+$.

This reaction requires the polysulfide (S_xS^{2-}) to be reduced by hydrogen sulfide (HS^-) to yield pyrite (FeS_2) and hydrogen ions (H^+), and reduced polysulfide. The first reaction

is thought to create framboidal crystals in the long term. The second reaction is an ion exchange, which could be carried out by SRB. It was suggested that these reactions played a role linking elemental sulfur to pyrite in Archean samples (Ono et al. 2009; Farquhar et al., 2013; Rickard, 2014).

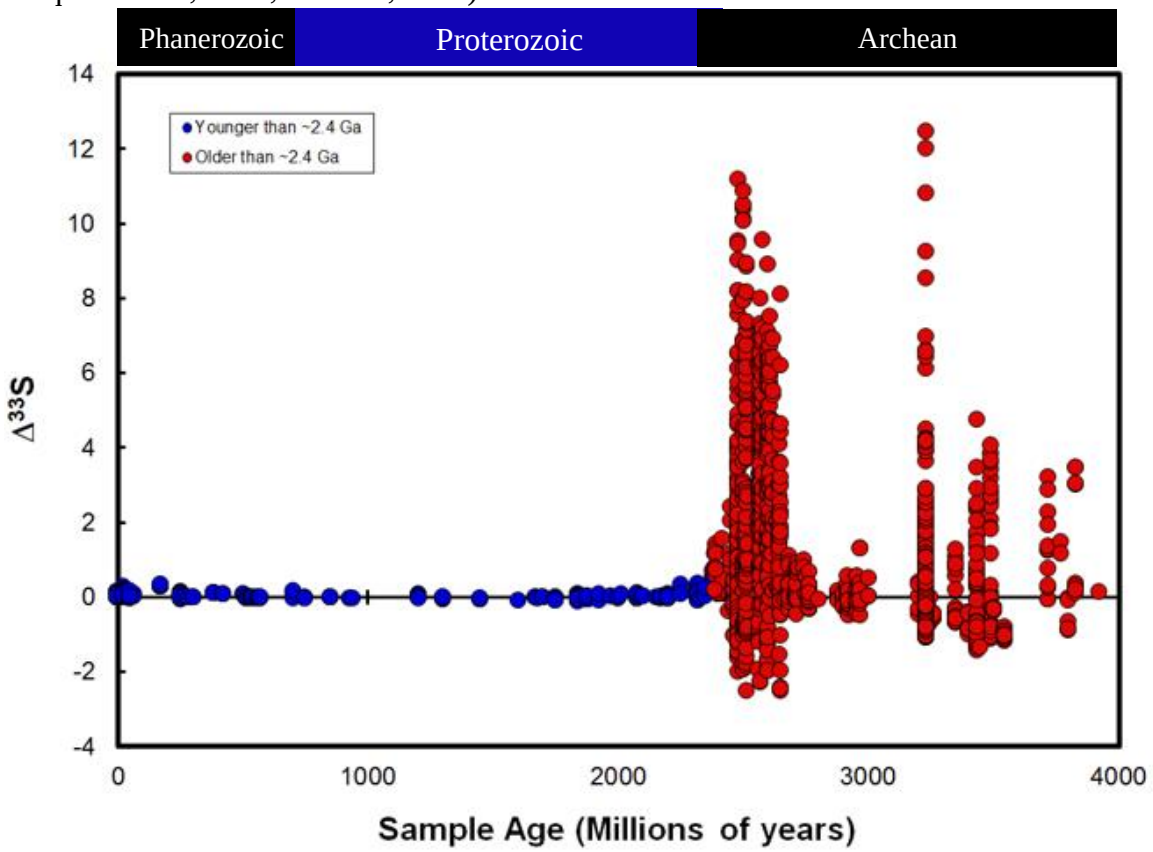

Figure 2. The y-axis is the $\Delta^{33}S$ and the x-axis is sample age of sedimentary rocks (from Farquhar compilation, pers. com, 2017). The general trend follows a horizontal line from Phanerozoic through Proterozoic Eon, then reaches the Archean Era and there are positive and negative $\Delta^{33}S$ signals, however, the signals are more positive than negative.

Hypothesis and Null Hypothesis

The experiments performed as part of this study involved sulfate reducing bacterial cultures that produced sulfide and iron sulfide minerals and consumed sulfate. Products formed and reactants remaining in these experiments was analyzed for their sulfur isotopic compositions to determine sulfur isotope fractionation signals. In this project, I test whether ***the experimentally produced pyrite will have a $\Delta^{33}S$ that is not the same as the $\Delta^{33}S$ of sulfate, but approaches the $\Delta^{33}S$ of elemental S (S°).*** If this is shown it will implicate S° or exchange between S° and sulfide produced by sulfate reduction in the pyrite or iron sulfide formation. Alternatively, the null hypothesis was: ***The experimentally produced pyrite will have the same $\Delta^{33}S$ as the residual sulfate and different from the elemental sulfur,*** which will rule out the possibility of isotopic

exchange between S° and sulfide produced by sulfate reduction, or of S° directly, in the pyrite or iron sulfide formation.

Methods and Materials

These hypotheses were tested experimentally using three types of experiments. In one type of experiment, bacteria grew in 100 mL serum bottles with chlorobutyl blue caps, under anoxic conditions. The cultures were in a medium of an artificial saltwater solution that supplied nutrients specific to the bacteria *Desulfobacterium autotrophicum* HRM2 with added elemental sulfur and added ferrous iron. The medium was adapted from a Navarrete et al (2010) slight modifications were made in order to work with the elemental sulfur and ferrous iron. The bacteria in the culture were added to the first set of experiments to see how SRB produced sulfide and reacts with S° and Fe^{2+} in the medium. In the second type of experiment (control #1), the bacteria was grown in the same way, but without added elemental sulfur. This control was designed to test the role of elemental sulfur and polysulfide formed by reaction of sulfide with elemental sulfur. In the third type of experiment (control #2), the same experimental design was used, but without bacteria. This control was designed to test the experiments in the absence of a source of hydrogen sulfide.

The organism, *Desulfobacterium autotrophicum* HRM2, is a marine sulfate-reducing bacterium that completely oxidizes Acetyl-CoA to carbon dioxide (CO_2). It is metabolically versatile can grow on CO_2 and can grow using H_2 and CO_2 under anoxic conditions. It is a chemolithoautotroph mesophilic, meaning it is an organism that grows in low-to moderate-temperature environments, and it does not grow well in cold or hot environments. This specific species HRM2 grows best between 0° to 31°C and prefers a pH of 6. The HRM2 species was used because it can adapt to minor changes in pH and temperature, and can feed off CO_2 or H_2, making it very useful for laboratory experiments.

The experiments included an oxidation-reduction indicator added to the medium to determine if, after autoclaving or during the course of the experiment, the medium is oxidized or reduced. The medium made was then transferred using nitrogen and carbon dioxide gas (N_2/CO_2) to pressurize the bottles at the same time. Once the medium was transferred, the serum bottles with the medium inside were placed in the autoclave and then heated to 121°C for twenty minutes. After the autoclave was finished and the samples were cooled, they were injected via needle and syringe with 0.1 mL of sterilized trace metal solution (SL-10). The trace element solution recipe that is used came from Brysch et al (1987). The SL-10 in one liter consists of 10 mL 7.7 M HCl, 1.5 g $FeCl_2 \cdot 4H_2O$, 70 mg $ZnCl_2$, 100 mg $MnCl_2 \cdot 4H_2O$, 6 mg H_3BO_3, 190 mg $CoCl_2 \cdot 6H_2O$, 2 mg $CuCl_2 \cdot 2H_2O$, 24 mg $NiCl_2 \cdot 6H_2O$, and 36 mg $Na_2MoO_4 \cdot 2H_2O$. Then, 0.1 mL of the Wolfe vitamin solution was injected. The Wolf vitamin solution consists of: 0.01 g/L pyridoxine • HCl, 5 mg/L thiamine • HCl, 5mg/L riboflavin, 5 mg/L nicotinic acid, 5 mg/L calciumpantotenate, 5 mg/L p-aminobenzoicacid, 2 mg/L biotin, 2 mg/L folic acid and 0.1 mg/L of cyanocobalamine. Lastly, 0.1 mL of sodium selenite was added to the bottles. Finally, the bottles were inoculated with 5 mL of bacteria culture, to start growing the set of cultures. Some of the culture mediums remained slightly pink,

implying that the medium was not fully reduced. Several cultures needed to be inoculated a second time with another 5 mL of bacterial culture in order to fully reduce. Once the cultures were stable and fully reduced, autoclaved sterilized ferrous chloride ($FeCl_2$) was added using a filter sterilized needle and syringe to inject. The expected life of the samples is from four to six weeks.

Spectrophotometry was performed three times to test for increase in cell mass of the bacteria. The spectrophotometer measures the turbidity or optical density, which is the measure of the light absorbed by bacterial suspension. The minimum absorption of this bacteria culture is six-hundred nanometers (600 nm) based on general microbiology.

The Cline solution method was used to determine the amount of dissolved hydrogen sulfide (H_2S, HS^-, S^{2-}) in a concentration range of 1.0-1000 micromoles per liters (μmol-atoms/L). The samples were diluted to a 2:25 ratio to get proper results. Using 900 μL of deoxygenated water, 1.0 mL of sample, 87 μL of the pre-made Cline solution into a 1.5 microcentrifuge tube and mixed gently by inverting the tube five times. After that, the tubes sat for twenty minutes. Then, the solution was transferred to the spectrophotometer cuvettes to run the analysis. Analyses were conducted at a wavelength of 670 nm (Cline, 1969). The first sample was a blank, and the results were compared to previously run Cline data. When in the presence of sulfide, the sample turns a yellow (high count) to a blue-green (low-count) color indicating some form of free sulfide is present.

The procedure to extract sulfide, was completed by removing 5 mL of culture with a sterile needle and syringe. The culture was pushed through a sterile filter syringe into a 15 mL conical centrifuge tube with 5 mL zinc acetate to capture the sulfide. From this solution, the sulfide was precipitated on the bottom as a white clump, while SO_4^{2-} remained in solution. The culture solution was separated and lied on top of precipitated sulfide, and then was taken out and disposed of to filter the sulfide, 10 mL of the solution was put in a separate 15 mL conical tube with 5 mL of barium chloride solution ($BaCl_2$). This precipitated sulfate as barium sulfate ($BaSO_4$) as a solid, which also had excess remaining culture solution that had to be pipetted out and disposed of, and then rinsed with milliQ water and spun down in the centrifuge for further separation.

In order to isolate S° samples were mixed with chloroform ($CHCl_3$). $CHCl_3$ is a toxic chemical that can react with a variety of materials including the nitrile gloves and represents a health hazard. Thus, $CHCl_3$ extractions undertaken in a fume hood with triple nitrile gloves. Cultures are 100 cc (cubic centimeter) with 0.18 grams (g) of elemental S, so using 3 x 10 cc (30 mL) of chloroform dissolved all elemental S. Once the 30 mL of $CHCl_3$ was injected into all four 100 mL culture bottles, culture bottles inverted and placed in glass beakers and left to sit overnight. The $CHCl_3$ dissolved elemental sulfur and separated it from the iron sulfur. The $CHCl_3$ was evaporated in a boiling flask to leave the elemental sulfur. Once elemental sulfur was removed, the precipitates were collected using vacuum filtration and washed with 20 mL of methanol (MeOH). As a precaution, after operations with $CHCl_3$ were completed, the hoods were left to evacuate volatiles overnight.

Mass spectrometry analysis

In order to obtain multiple sulfur isotope data on my experiments, I analyzed precipitated silver sulfide (AgS) on a mass spectrometer. The mass spectrometry combusts silver sulfide (Ag_2S) samples, ionizes them. The ion beam is focused and travels past a magnet where the isotopes are separated by mass. The ratios of the isotopes 34/32 sulfur were collected and measured on faraday cups. To date all data for δ^{33}, δ^{34}, and $\Delta^{33}S$ have been completed with the exception of group #2 of the twelve experiments.

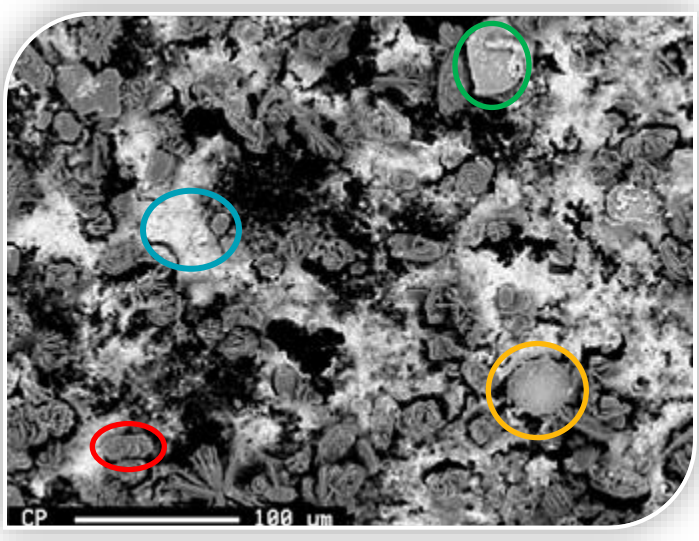

Figure 3 backscattered electron image of sediment from initial experiments. Sample #6, contains bacteria, ferrous, and elemental sulfur

EPMA

Precipitates from experiments were studied by using a JEOL 8900 Electron Probe Microanalyzer (EPMA) at the Advanced Imaging and Microscopy Laboratory (AIMLab) at the Maryland Nanocenter. Energy Dispersive Spectroscopy was performed to obtain a qualitative assessment of the chemistry of precipitates from the cultures. To prepare samples, approximately 5 mL of culture was extracted using a syringe and filtered using a filter chimney and vacuum flask. The precipitate was carefully placed on carbon tape adhered to a glass slide, labeled, and coated with carbon.

Results of 393 work

Electron microprobe analysis of the precipitates revealed spheres of elemental sulfur (yellow circle), white web looking material is iron sulfide (blue circle), and the oyster shell looking material is iron phosphorous mineral (red circle), and the flat light gray platy crystal is the iron sulfide (green circle), (Fig. 3). Compositional data were collected using energy-dispersive spectrometry (EDS) and Backscattered electron image (BSE). The EDS spectra collected were consistent with the presence of pyrite and an iron sulfur mineral (Fig. 4) in all four cultures with bacteria present. In addition, to the pyrite and iron sulfur, there is an iron phosphate mineral in the cultures, more analysis will need to be completed to determine which iron phosphorous mineral it is.

Among the four experiments conducted in this study, sulfide abundance varied. No free sulfide was extracted using zinc acetate from the first experiment that consisted of

four cultures, reflecting formation of iron sulfide. However, there was low-levels of aqueous sulfide generated and observed. Using the Cline method, which turns the sample blue-green in the presence of sulfide. After, analyzing the samples using the spectrophotometer, the absorbance of 0.949 nanometers (nm) (shown in table #1) supports the presence of sulfide in solution. In the second experiment of the set of 12 samples showed that there was a depletion of free sulfide generated in the groups with no elemental sulfur, and little sulfide in group four. The reason for depletion in group 4 is likely due to the bacteria consuming and production of pyrite formation. Group #2 with no Fe^{2+}, generated the most free sulfide and has a potent smell of rotten eggs indicating sulfide is present in abundance. This data adds additional evidence to support the first claim with the initial experiments (see table #3).

Table #2, initial experiments Cline results

Sample # and contents in sample	Absorbance
#1, salt solution & Fe^{2+}	0.086
#2, bacteria, Fe^{2+}, and S°	1.147
#3 salt solution, Fe^{2+}, and S°	0.103
#4, bacteria, Fe2+, and S°	0.949

The method for extracting sulfate was successful all four cultures had enough precipitate for extraction to be run later using the mass spectrometer. Elemental sulfur was extracted from all cultures that contained elemental sulfur. Iron sulfide sulfur (pyrite) was present in all cultures with bacteria, but none was present in the abiological control (control #2). This indicates that the microbes reduced sulfate to form sulfide, which reacted with ferrous iron to form iron sulfide. The greatest amount iron sulfide was found in the ones with elemental sulfur and bacteria and a lower amount found in the one without elemental sulfur. This supports the hypothesis that sulfur plays a role in pyrite formation.

Mass spectrometry analyses (see below, fig 4), the x-axis shows the values of $\delta^{34}S$. the iron sulfide formed in experiments with S° does not have strongly negative $\delta^{34}S$. Thus, demonstrating a role for elemental sulfur in iron sulfide isotopic composition. The -19.49 is a small part of the total sample and may be FeS rather than FeS_2. If it is FeS it provides interesting insight into the pathways for forming iron sulfides. Samples labeled "A" were not heated. Whereas, samples labeled "B" were heated, so the "B" labeled samples produced FeS_2 over FeS. The samples labeled "A" will also produce FeS_2, but slowly, and these samples reacted quickly. FeS Reacts quickly without heat so it is likely it is FeS, but this is something that will need to be (and is planned to be) tested. Only delta ^{34}S analyses have been run, the initial observations, the data samples with elemental

sulfur are less negative (-), than the samples without elemental sulfur, which in return have very negative values (-).

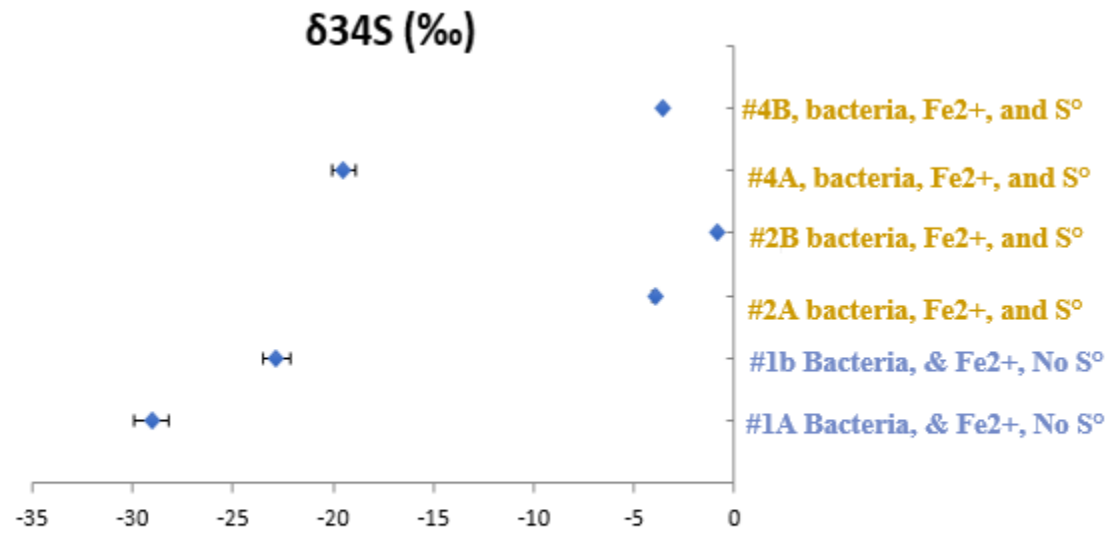

Figure 4. Cal tech plot of $\delta^{34}S$ isotopic data, error bars are +/- 0.3‰. The samples labeled "A": is the AgS extracted with gas, could be FeS instead of FeS2, which might be formed from the sulfide directly not the elemental sulfur that needs to be tested, but it will be tested. First extracts are more negative (-). The samples labeled "B": is the AgS from heat

Electron microprobe analysis of the precipitates revealed spheres of elemental sulfur, iron sulfide, and an iron phosphorous mineral (Fig. 3). Compositional data were collected using energy-dispersive spectrometry (EDS) and Backscattered electron image (BSE). The EDS spectra collected were consistent with the presence of pyrite and an iron sulfur mineral (Fig. 5) in all four cultures with bacteria present. In addition, to the pyrite and iron sulfur, there is an iron phosphate mineral in the cultures, more analysis will need to be completed to determine what iron phosphorous mineral it is.

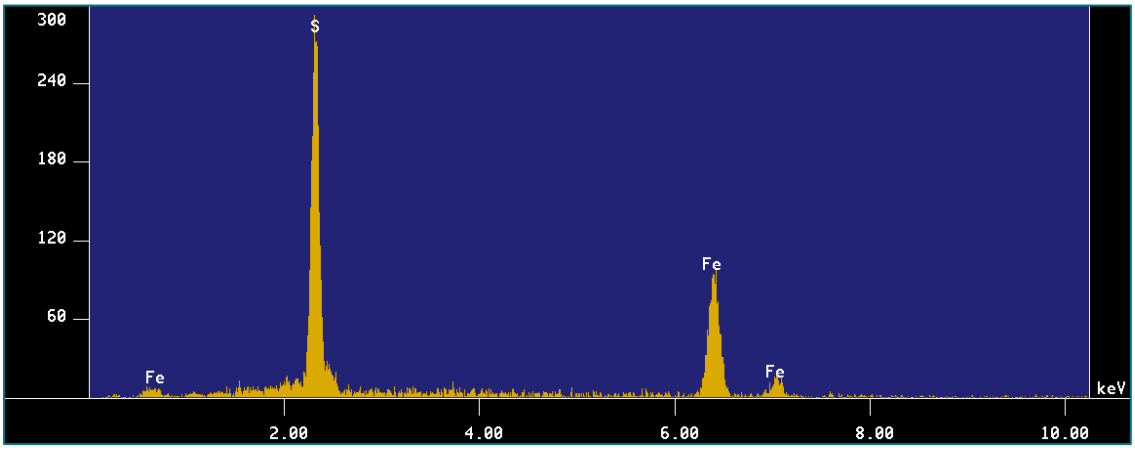

Figure 5. Energy dispersive spectroscopy (EDS) spectrum exhibiting a high concertation of iron and sulfur in the experiment run products, sample 6 – bacteria, Ferrous, and S° culture.

Results of 394 work

Table 3 presents the results of Cline analyses. Group #1 yield absorbance values to that of the blank indicating no sulfide accumulation. Which is accurate because there is no bacteria present, so no free sulfide should be present. This also means that the chemistry of the experimental design is correct. However, group 2 yield absorbance values indicating sulfide accumulation. This group smelled of rotten eggs, so it was expected to get a high amount of free sulfide. The general color of this aqueous solution was yellow, which is the general color for polysulfide species. Unfortunately, for groups #3 and #4 yield absorbance values indicating little to no sulfide accumulation. This is because the bacteria produce the free sulfide, however, free sulfide reacts quickly with ferrous iron to form FeS.

Table #3, experiments in triplicate Cline results

Sample #	Absorbance
Blank	0.051
Group #1, a	0.053
Group #1, b	0.054
Group #1, c	0.056
Group #2, a	0.196
Group #2, b	0.210
Group #2, c	0.260
Group #3, a	0.076
Group #3, b	0.059
Group #3, c	0.069
Group #4, a	0.063
Group #4, b	0.058
Group #4, c	0.059

Table #4 and appendix table A3 present the isotopic data for the four experiments. The initial sulfate has an average $\delta^{34}S$ of 16.0‰, a $\delta^{33}S$ of 2.9‰, and a $\Delta^{33}S$ of 14.5‰. The idea was to have a $\Delta^{33}S$ of labeled SO_4^{2-} that is different from the $\delta^{33}S$ of S°. The target $\Delta^{33}S$ for SO_4^{2-} was 10‰. There was an unknown amount of SO_4^{2-} with $\Delta^{33}S = 0$ mixed in the aqueous SO_4^{2-} salt solution with $\Delta^{33}S = 14$. The high $\Delta^{33}S$ of SO_4^{2-} in group #1 experiments had the highest $\Delta^{33}S$ because it was not diluted by inoculation with solution containing SO_4^{2-} with $\Delta^{33}S = 0$. This experiment also generated no sulfide or FeS/FeS_2. This is expected because there are no bacteria present, so there is no generating of free sulfide to exchange and or react, so there is no exchanging of $\Delta^{33}S$ it is just a chemistry control. In general, the sulfate in experiments with bacteria have lower $\Delta^{33}S$

(closer to 0) because the signature of biological material injected with the inoculation had $\Delta^{33}S$ equal to zero, and this dilutes and lowers the $\Delta^{33}S$. The SRB prefer ^{32}S; so, the product sulfide has a negative $\delta^{34}S$, and the residual SO_4^{2-} will have a more positive $\delta^{34}S$. Elemental sulfur in all experiments had a $\delta^{33}S$ of ~3.9‰, a $\delta^{34}S$ of 6.7‰, and this S° had a different $\Delta^{33}S$ that was surprisingly not zero, but instead a $\Delta^{33}S$ of 0.5‰. The values for S° are from group one because it is simply just the chemistry check. Iron sulfides (FeS and FeS_2) plot along a linear relationship with more negative $\delta^{34}S$, than both sulfate and elemental sulfur and that tends toward the composition of the elemental sulfur and to more negative $\delta^{34}S$ than the sulfate (See Figure 6-8, and 11 below). The reason for this is in sulfate reduction, the product sulfide is depleted in minor sulfur isotopes compared to the major sulfur isotope (^{32}S).

Table 4: Average values from experiments

Experiment	Species		$\delta^{33}S$	$\delta^{34}S$	$\Delta^{33}S$
	initial sulfate	average	16.0	2.9	14.5
		std dev	0.4	0.1	0.4
	Control: No biology (Fe(II), Sulfate, Elemental S)				
1A	Elemental S	average	3.9	6.7	0.5
		std dev	0.3	0.6	0.1
1A	Sulfate	average	15.7	3.3	14.0
		std dev	0.3	0.2	0.3
	No Fe(II): Biology, Sulfate, Elemental S				
2A	Elemental S	average	5.2	9.1	0.5
		std dev	0.1	0.1	0.1
2A	Sulfate	average	17.1	8.9	12.5
		std dev	1.3	1.8	0.7
	No Elemental S: Biology, Sulfate, Fe(II)				
3A	AVS	average	2.3	-18.7	12.0
		std dev	0.3	4.6	2.1
3A	CRS	average	3.4	-16.1	11.7
		std dev	0.7	3.5	**1.3**
3A	Sulfate	average	17.5	11.7	11.5
		std dev	1.1	2.7	**1.5**

Table 4 (contd) : Average values from experiments

Experiment	Species		$\delta^{33}S$	$\delta^{34}S$	$\Delta^{33}S$
		Biology, Sulfate, Elemental S, Fe(II)			
4A	AVS	average	2.8	-14.3	10.2
		std dev	0.3	1.1	0.3
4A	CRS	average	3.4	-6.4	6.7
		std dev	0.3	3.1	1.4
4A	Elemental S	average	4.7	5.9	1.7
		std dev	0.2	2.0	0.8
4A	Sulfate	average	18.8	14.4	11.4
		std dev	3.1	5.4	0.5
		Reference materials			
NBS 127	Reference	average	10.9	21.1	0.0
		std dev	0.1	0.2	0.1

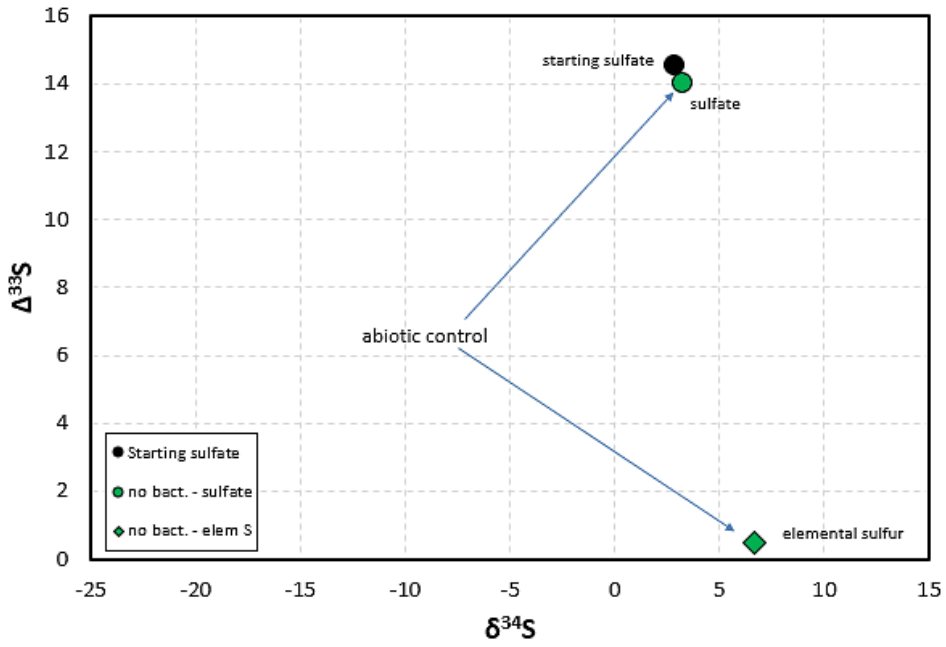

Figure 6, displays starting sulfate (black dot), with sulfate of group #1 (abiological control).

Figure 6, displays values of the initial sulfate and the sulfate of group #1 (abiological control) which are about the same value. The group #1 the elemental sulfur (green diamond), displays the starting S° of the experiment. Error bars are too small to be seen.

Discussion

The twelve experiments have been successfully run, table #4, above, displays the drift correction, normalized to Canyon Diablo Troilite (CDT). In table #4 the first group the sulfate and elemental S do not exchange, and chemical separation of sulfate and elemental sulfur is effective. The reproducibility of the experiment is valid and reproducible for techniques. The elemental S appears to have a nonzero $\Delta^{33}S$, it is possibly due to normalization procedure and mass spectrometry.

In group #2, (green) (no Fe^{2+}) there was ample amounts of produced polysulfide and had residual elemental S. The polysulfide isotopic composition was not measured, but its presence was documented with Cline and it was seen as a yellow coloration of the solution.

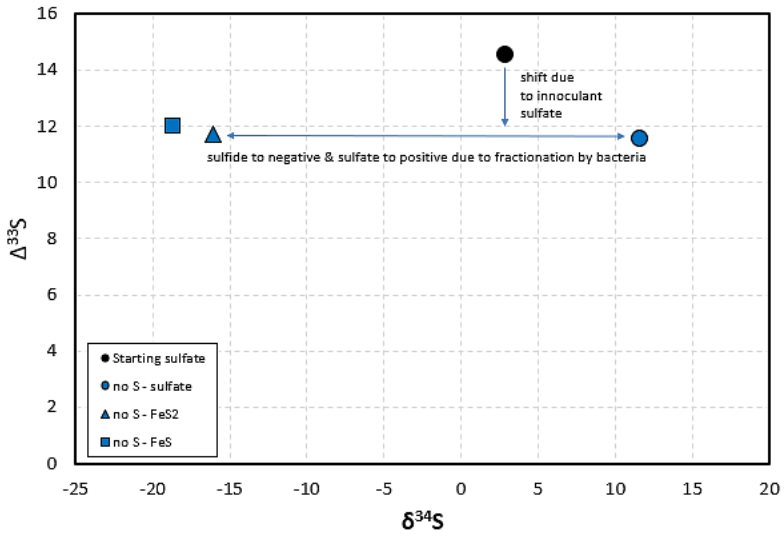

Figure 7, displays starting sulfate (black dot), with sulfate of group #3 (blue dot).

In figure 7, there is a shift down to lower $\Delta^{33}S$, from the inoculation of bacteria. The FeS (blue box: group #3 (no elemental S)) generated from ARS shifts to a more negative value of $\delta^{34}S$, due to a depletion in minor isotopes from reaction mechanism, no exchange to lower $\Delta^{33}S$ is seen for FeS and FeS_2. The FeS_2 (blue triangle) formed from CRS (chromium II sulfide) is a similar value to that of the FeS for the same reason. Error bars are too small to be seen. There is a shift to positive $\delta^{34}S$ for sulfate because the MSR leaves excess amount of ^{34}S.

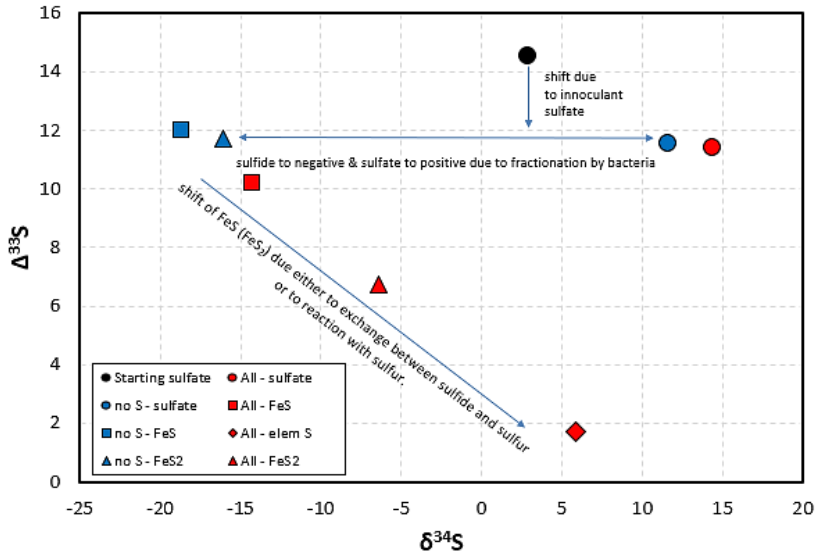

Figure 8, displays starting sulfate (black dot), with sulfate of group #3 (blue dot), along with sulfate of group #4 (red dot).

In figure 8, (group #3 blue/group #4 red) there is a shift down in both groups, from the inoculation of bacteria and a shift to a more positive $\delta^{34}S$ due to depletion in $\delta^{33}S$ because it is preferential for the bacteria. The FeS (blue box) generated from ARS shifts to a more negative value of $\delta^{34}S$, due to a depletion in minor isotopes from reaction mechanism, no exchange is seen. However, for group #4 the FeS (red square) formed from AVS (acid-volatile sulfides) the same shift to the left is seen and a shift down to a value closer to 0, there is possibility of not only reacting but also an exchange reaction occurring.

In group #4 (system with both Fe(II) and elemental S), sulfate reduction produces AVS (FeS) and CrS (FeS_2). The AVS may have a $\Delta^{33}S$ that is closer to sulfate but may show a small shift. The variance is large and overlaps with sulfate. However, the CrS has a value in between sulfate and elemental S, indicating a role for elemental S in CrS formation. The possible difference between CrS and AVS (they overlap) might indicate the polysulfide (or elemental S) pathway is active in the experiment rather than direct exchange between sulfide and elemental sulfur by way of polysulfide (if elemental sulfur exchanged, it would transmit the same signal to AVS and CRS (this is small number of data points and needs further testing). It appears that in group #4 there is both proposed reactions (1 & 2: motivation section of thesis) occurring. Implications of reactions 1 and 2 are: if Fe(II) and Elemental S are present then the signal will carry part of the elemental S. There is small reduction of $\Delta^{33}S$ of sulfate (may indicate some polysulfide oxidation).

Implications for the Archean, if the conditions were like group #3 (no elemental S), sulfate reduction and chemistry would have produced both AVS (acid-volatile sulfides) (most likely FeS species) and CrS (chromium II sulfide) (could be FeS_2), similar to what would be expected in nature. The $\Delta^{33}S$ was transferred from sulfate to both AVS and CrS species. The implication for Archean, if no elemental S the sulfide will have same $\Delta^{33}S$ as sulfate. If the conditions were like group #4 (system with both Fe(II) and elemental S), sulfate reduction and chemistry would have produced both AVS (most likely FeS species) and CrS (could be FeS_2) with $\Delta^{33}S$ values between sulfate and elemental sulfur.

Conclusion and Broader Impacts

One goal of this work was to create a culture that has pyrite or another iron sulfide precipitate. This has been accomplished and the iron-sulfide products have been confirmed by using EDS with the electron probe microanalyzer. These analyses showed additional complexity in the form of an iron phosphorous mineral (Figure 10). In addition, above figure 5 shows the energy dispersive spectra with a high concentration of iron and sulfur that looks qualitatively like the standard for pyrite (see below, Figure 11).

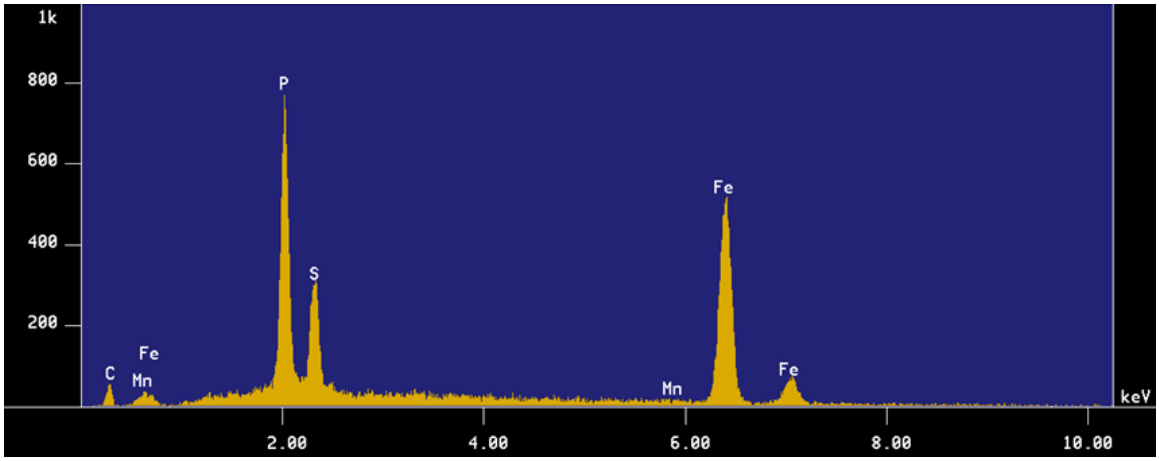

Figure 10, Energy dispersive spectroscopy (EDS) spectrum exhibiting a high concertation of iron and phosphate in the experiment, sample #4 containing bacteria, ferrous iron, and S°.

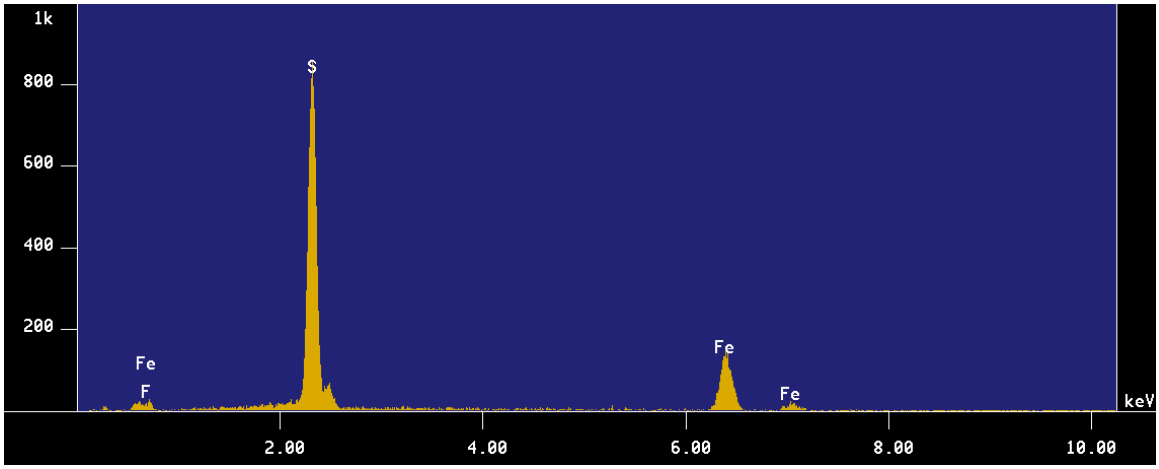

Figure 10, Energy dispersive spectroscopy (EDS) spectrum exhibiting a pyrite standard.

A second goal of this work was to show that hydrogen sulfide was produced and used in the making of iron sulfide (pyrite) mineral. This was accomplished. The experiment with no bacteria produced no hydrogen sulfide and no iron sulfide, but the other ones did.

A third goal of this work was to show the hydrogen sulfide reacts with elemental sulfur to form polysulfide and then that reacts to form pyrite. This has been accomplished. Experiments conducted with S° produced more iron sulfides versus those without S° (samples #2 and #4 see below, Table #5).

Table #5, Samples from initial experiments

Sample # and contents in sample	Total mass
#1, aqueous SO_4^{2-} salt solution, & Fe^{2+}	3.647 mg
#2, aqueous SO_4^{2-} salt solution, bacteria, Fe^{2+}, and S°	13.2 mg
#3 aqueous SO_4^{2-} salt solution, Fe^{2+}, and S°	0.1165 mg
#4 aqueous SO_4^{2-} salt solution, bacteria, Fe2+, and S°	8.361 mg

A fourth goal of this work was to show that the isotopic signals from elemental sulfur in experiments are related to the signals found in the iron sulfide (pyrite) in experiments. This has not been accomplished. I am waiting to run analyses.

To summarize, the experiment was to come up with ways to test the hypothesis that elemental sulfur takes part in the mechanism to form pyrite, by reacting with bacterial hydrogen sulfide. A second type of experiment was conducted for the second term. The bacteria were grown in the same way in a series of four experiments. Below in figure 11, displays the reaction mechanisms of the low-temperature pyrite formation experiments that underwent for this senior thesis. In figure 11, there is a shift down in the three groups (#2, #3, & #4), from the inoculation of bacteria and a shift to a more positive $\delta^{34}S$ due to depletion in $\delta^{33}S$ because it is preferential for the bacteria. The FeS (blue box) generated from ARS shifts to a more negative value of $\delta^{34}S$, due to a depletion in minor isotopes from reaction mechanism, no exchange is seen. Group #4 the FeS (red square) formed from AVS the same shift to the left is seen and a shift down to a value closer to 0, there is possibility of not only reacting but also an exchange reaction occurring. The FeS_2 (blue triangle) of group #2, formed from CRS is a similar value to that of the FeS for the same reason. The group #4 FeS_2 (red triangle) has a greater shift down and to the right, closer to the value of the S°, so here there is a role for S° in an exchange reaction. For group#2 extraction of S° (yellow diamond) was collected and plotted in this plot to show reproducibility and accuracy. Error bars are too small to be seen.

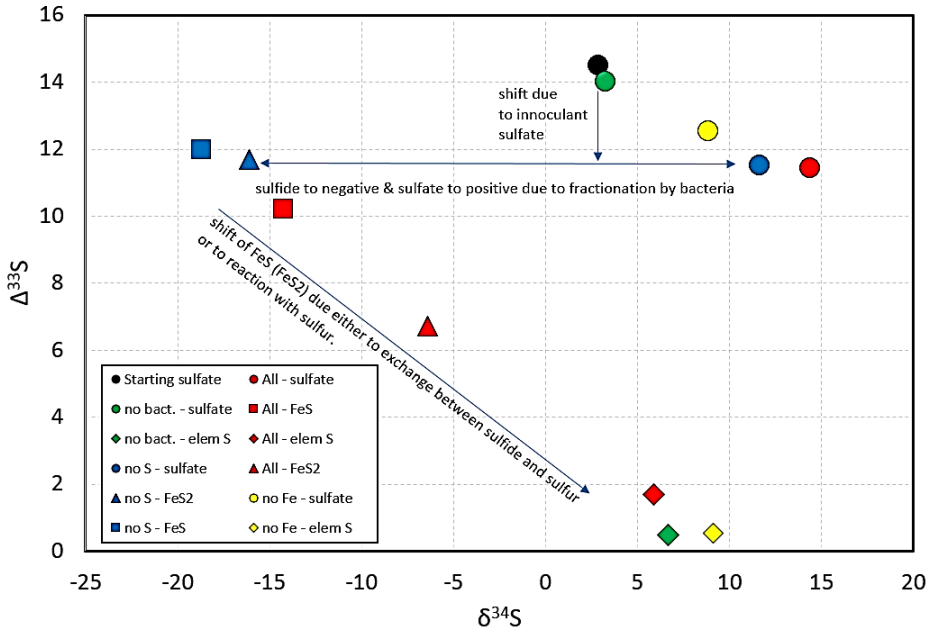

Figure 11, displays starting sulfate (black dot), with sulfate group #3 (blue dot), sulfate of group #4 (red dot), and sulfate group #2 (yellow dot).

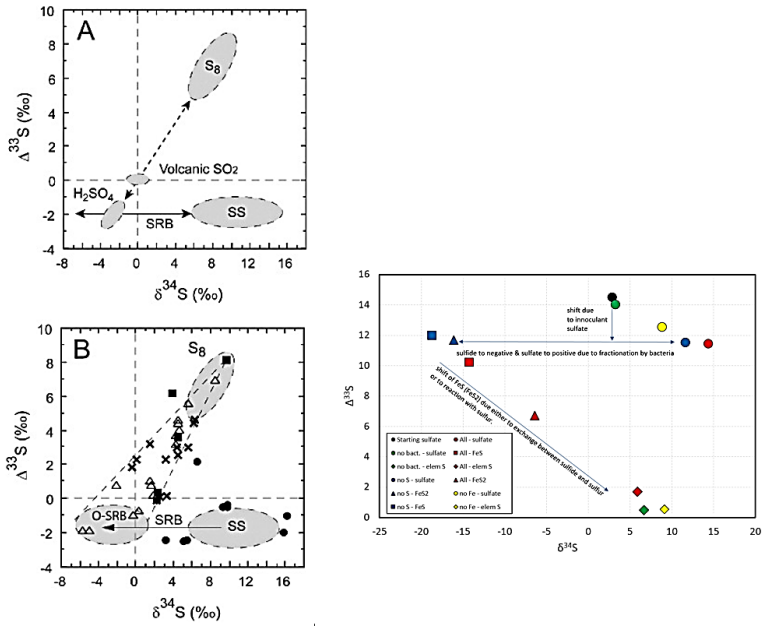

Figure 12, on the left is two plots (A & B) by Shuhei Ono(2003), and on the right is figure 11. In Ono's plot the S8 is elemental sulfur, the SS stands for seawater sulfate, and the O-SRB represents estimated field of pyrite formed by bacterial sulfate reduction in a pelagic environment.

Figure 12 above, displays three plots. The two on the right (plot A & B) are by Shuhei Ono (2003), and the plot on the right is figure 11(above). The schematic that Ono designed are the exact same as my final plot except in reverse. I used a + $\Delta^{33}S$ label for

the SO_4^{2-}, and the $\Delta^{33}S$ of the S° is 0.5 ‰. Ono set his plot up showing that there is S° displaying positive values on the top with $\Delta^{33}S$ values ranging from 4.5-8 ‰, and the starting SO_4^{2-} on the bottom right with a $\Delta^{33}S$ value of ~(-3)-(-1)‰. Ono's plot displays initial SO_4^{2-} on the bottom right making a shift to the right with inoculation of SRB, and then forming iron sulfide products with a value closer to that of S°.

The proposed mechanism was that in the presence of S° the pyrite formed would have a $\Delta^{33}S$ value that nears to that of S°. In figure 11 it shows just that the red triangle has a value closer to the elemental sulfur values obtained from this experiment, indicating a role for S° just like in the Archean Eon (figure 12). Figure 11, also displays the value of the pyrite (blue triangle) formed in the absence of S°. This value shows a value similar to that of the FeS (blue square) formed, indicating that without S° there is no exchanging, only reactions. Results similar to this are in the paper by Zhelezinskaia et al. 2014 in carbonates which had low elemental sulfur.

Suggestions for Future Work

To run a low temperature pyrite formation experiments that have excess amounts of S° and a limited abundance of Fe^{2+}. To try to possibly determine exactly how much Fe^{2+} would have been needed to form pyrite during the Archean Eon. Additionally, changing the design of the experiment such as using a sterile anoxic chamber to be sure that the environment remains to that of the Archean, and reduce the likelihood of contamination. The results produced from the isotopic data have little variation indicating reproducibility, so instead of focusing on the reaction mechanisms and exchange of isotopic values during pyrite formation, it would be interesting to focus more on the bacteria. How much energy is needed for growth, what are the most favorable conditions, and the life expectancy of the cells in a large volume verse a smaller volume. Additionally, this may lead to understanding how the overall mechanism involving SRB works and answer questions such as what is the enzyme that forms to act as a catalyst to make this biochemical reaction happen, and is there more than one? Does this specific SRB have the capability to potentially to enzymatically reduce Fe (III) and/or U (VI), and if it can could these bacteria possibly be found in a deep-water reservoir on a planetary body? The low temperature pyrite formation experiments that underwent was just a start paving a pathway to continue with more insightful experiments and gaining more knowledge to the evolution of the Earth.

Acknowledgements

My advisers, Dr. James Farquhar and James Dottin, III. My co-analytical adviser Dr. Alan J Kaufman for use of his mass spectrometer and the assistance in the data collected. The Paleoclimate Co-laboratory. The continuous Support of the NSF, Agouron Institute, and internal lab funds. Dr. Phil Piccoli for not only taking the time to allow the use of the JEOL 8900 Electron Probe Microanalyzer (EPMA) at the Advanced Imaging and Microscopy Laboratory (AIMLab) at the Maryland Nanocenter, but also proofing and edits.

Appendix

Table A1 Uncorrected mass spectrometer results

Sample Number	Name	Acquisition date	RT (Sec)	Height (nA)	Type	Weight (mg)	Sample Description	S33	S34		Elemental Composition
SampleNo/s	DataFileName/s	AcquisitionDate/s	RetTimeSecs	Major Height nA	SampleType/s	Sample Weight/s	SampleDescription/s	DisplayDelta1	DisplayDelta2	SMOW Converted	R_1EC
8	04242018_NBS127_R4.raw	24/4/18 8:58	177.2	1.50	Elem	0.19		4.56	12.85	43.71	10.95
9	04242018_NBS127_R5.raw	24/4/18 10:49	176.8	1.70	Elem	0.19		5.26	13.13	43.99	11.09
10	04242018_NBS127_R6.raw	24/4/18 12:24	176.2	1.93	Elem	0.19		5.42	12.58	43.44	12.40
11	04242018_NBS127_R7.raw	24/4/18 12:37	176.0	2.49	Elem	0.22		5.56	12.79	43.65	13.19
12	04242018_NBS127_R8.raw	24/4/18 12:42	175.4	2.24	Elem	0.20		5.56	12.54	43.40	13.19
13	04242018_NBS127_R9.raw	24/4/18 12:48	176.3	2.08	Elem	0.18		5.34	12.35	43.21	13.15
14	04242018_LP_3ACRS.raw	24/4/18 12:56	175.8	1.94		0.20		-2.69	-28.00	2.86	11.31
15	04242018_LP_4AARS.raw	24/4/18 13:01	176.0	2.10		0.19		-2.26	-21.68	9.18	12.82
16	04242018_LP_4ACRS.raw	24/4/18 13:07	175.7	2.42		0.22		-1.26	-10.67	20.19	12.88
17	04242018_LP_4ACRS2.raw	24/4/18 13:13	175.7	2.10		0.19		-2.01	-17.62	13.24	13.02
18	04242018_LP_2A1.raw	24/4/18 13:19	175.3	2.30		0.21		-0.10	1.06	31.92	12.33
19	04242018_LP_2A2.raw	24/4/18 13:24	175.4	2.23		0.19		0.08	0.91	31.77	13.54
20	04242018_LP_4A1.raw	24/4/18 13:30	174.9	2.65		0.22		-0.64	-3.55	27.31	13.70
21	04242018_LP_4A2.raw	24/4/18 13:36	175.4	2.61		0.21		-0.65	-3.43	27.43	13.71
22	04242018_LP_ARS1A.raw	24/4/18 13:52	175.1	2.47		0.20		-1.08	-1.23	29.63	13.49
23	04242018_LP_ARS1B.raw	24/4/18 13:58	175.1	2.55		0.20		-1.21	-1.35	29.51	13.65
24	04242018_NBS127_R10.raw	24/4/18 14:04	175.1	2.55	Elem	0.20		5.72	12.70	43.56	14.14
25	04242018_NBS127_R11.raw	24/4/18 14:09	175.1	3.01	Elem	0.21		5.74	12.57	43.43	15.21
26	04242018_LP_AVS3A.raw	24/4/18 14:15	175.0	2.78		0.22		-3.07	-30.02	0.84	13.71

27	04242018_LP_AVS3B.raw	24/4/18 14:21	175.5	2.39		0.19		-2.65	-23.50	7.36	13.44
28	04242018_LP_AVS3C.raw	24/4/18 14:27	174.6	5.53		0.21		2.34	-4.34	26.52	28.34
29	04242018_LP_3B CRS.raw	24/4/18 14:32	175.3	2.68		0.21		-1.56	-21.13	9.73	13.39
30	04242018_LP_4B ARS.raw	24/4/18 14:38	175.0	2.44		0.20		-2.52	-23.13	7.73	13.48
31	04242018_LP_4B CRS.raw	24/4/18 14:44	175.0	2.71		0.22		-1.84	-15.02	15.84	13.49
32	04242018_LP_4B CRS2.raw	24/4/18 14:50	175.5	2.30		0.19		-1.80	-18.56	12.30	13.83
33	04242018_LP_2B1.raw	24/4/18 14:56	174.4	2.54		0.20		0.03	1.09	31.95	13.90
34	04242018_LP_2B2.raw	24/4/18 15:01	174.7	2.66		0.20		0.12	0.80	31.66	14.04
35	04242018_LP_4B1.raw	24/4/18 15:07	174.9	2.82		0.21		-0.03	0.24	31.10	14.26
36	04242018_LP_4B2.raw	24/4/18 15:13	174.5	2.71		0.20		-0.27	0.02	30.88	14.17
37	04242018_NBS127_R12.raw	24/4/18 15:19	174.8	2.97	Elem	0.20		5.81	13.06	43.92	15.70
38	04242018_NBS127_R13.raw	24/4/18 15:25	174.5	2.69	Elem	0.22		5.66	12.78	43.64	12.89
39	04242018_LP_1C ARS.raw	24/4/18 15:30	174.5	2.46		0.22		-1.52	-2.25	28.61	12.47
40	04242018_LP_3C CRS.raw	24/4/18 15:36	174.8	2.73		0.20		-1.17	-23.45	7.41	14.33
41	04242018_LP_4C ARS.raw	24/4/18 15:42	175.2	0.68		0.06		-3.49	-20.19	10.67	11.39
42	04242018_LP_4C CRS.raw	24/4/18 15:48	175.1	2.30		0.18		-2.02	-12.97	17.89	13.76
43	04242018_LP_4B CRS2.raw	24/4/18 15:54	175.1	2.53		0.20		-1.56	-12.62	18.24	13.39
44	04242018_LP_2C1.raw	24/4/18 15:59	174.7	2.46		0.18		-0.22	0.33	31.19	14.21
45	04242018_LP_2C2.raw	24/4/18 16:05	174.5	2.93		0.22		0.00	0.81	31.67	14.19
46	04242018_LP_4C1.raw	24/4/18 16:11	174.8	2.76		0.22		-0.46	-3.64	27.22	13.73
47	04242018_LP_4C2.raw	24/4/18 16:17	174.6	2.65		0.20		-0.54	-3.86	27.00	13.96
48	04242018_LP_1A.raw	24/4/18 16:22	174.3	3.18		0.22		10.61	-4.73	26.13	15.54
49	04242018_NBS127_R14.raw	24/4/18 16:28	174.7	2.83	Elem	0.21		5.74	12.87	43.73	14.52
50	04242018_NBS127_R15.raw	24/4/18 16:34	175.0	3.10	Elem	0.22		5.71	12.95	43.81	15.28
51	04242018_LP_2A.raw	24/4/18 16:40	175.0	2.55		0.18		10.55	-0.88	29.98	14.98
52	04242018_LP_3A.raw	24/4/18 16:46	175.1	2.29		0.18		13.56	3.11	33.97	14.49
53	04242018_LP_4A.raw	24/4/18 16:52	175.1	2.86		0.20		11.88	2.45	33.31	15.33

54	04242018_LP_1B.raw	24/4/18 16:57	174.7	2.76		0.22		10.83	-5.06	25.80	13.43
55	04242018_LP_2B.raw	24/4/18 17:03	174.8	2.48		0.18		12.80	2.63	33.49	14.86
56	04242018_LP_3B.raw	24/4/18 17:09	174.7	3.03		0.22		12.35	6.41	37.27	14.89
57	04242018_LP_4B.raw	24/4/18 17:15	175.2	3.03		0.21		11.97	3.89	34.75	15.18
58	04242018_LP_1C.raw	24/4/18 17:21	175.0	2.51		0.20		10.34	-4.70	26.16	13.95
59	04242018_LP_2C.raw	24/4/18 17:26	175.3	2.67		0.20		12.71	0.50	31.36	14.84
60	04242018_LP_3C.raw	24/4/18 17:32	174.8	2.78		0.20		11.37	1.06	31.92	14.93
61	04242018_NBS127_R16.raw	24/4/18 17:38	174.8	2.53	Elem	0.19		5.78	12.59	43.45	14.79
62	04242018_NBS127_R17.raw	24/4/18 17:44	173.6	2.75	Elem	0.20		5.90	12.89	43.75	14.77
63	04242018_LP_4C.raw	24/4/18 17:50	175.0	2.51		0.18		17.35	12.44	43.30	15.34
64	04242018_LP_1 batch 1.raw	24/4/18 17:56	175.8	2.31		0.19		10.66	-5.23	25.63	13.25
65	04242018_LP_2 batch 1.raw	24/4/18 18:01	175.0	2.48		0.19		10.82	-5.11	25.75	13.92
66	04242018_LP_batch 3.raw	24/4/18 18:07	175.3	2.39		0.18		11.42	-5.09	25.77	14.03
67	04242018_NBS127_R18.raw	24/4/18 18:13	175.5	2.65	Elem	0.20		5.82	13.00	43.86	14.83

Table A2 Standard Data for Calculating corrections

Date and time	$\delta^{33}S$	$\delta^{34}S$	$\Delta^{33}S$
4/24/18 12:28 PM	5.42	12.58	-1.03906
4/24/18 12:43 PM	5.56	12.79	-1.00655
4/24/18 12:43 PM	5.56	12.54	-0.87858
4/24/18 12:43 PM	5.34	12.35	-1.00132
4/24/18 2:09 PM	5.72	12.7	-0.80048
4/24/18 2:09 PM	5.74	12.57	-0.71394
4/24/18 3:21 PM	5.81	13.06	-0.89474
4/24/18 3:21 PM	5.66	12.78	-0.90143
4/24/18 4:33 PM	5.74	12.87	-0.86749
4/24/18 4:33 PM	5.71	12.95	-0.93844
4/24/18 5:45 PM	5.78	12.59	-0.68418
4/24/18 5:45 PM	5.9	12.89	-0.71773
4/24/18 6:14 PM	5.82	13	-0.85403

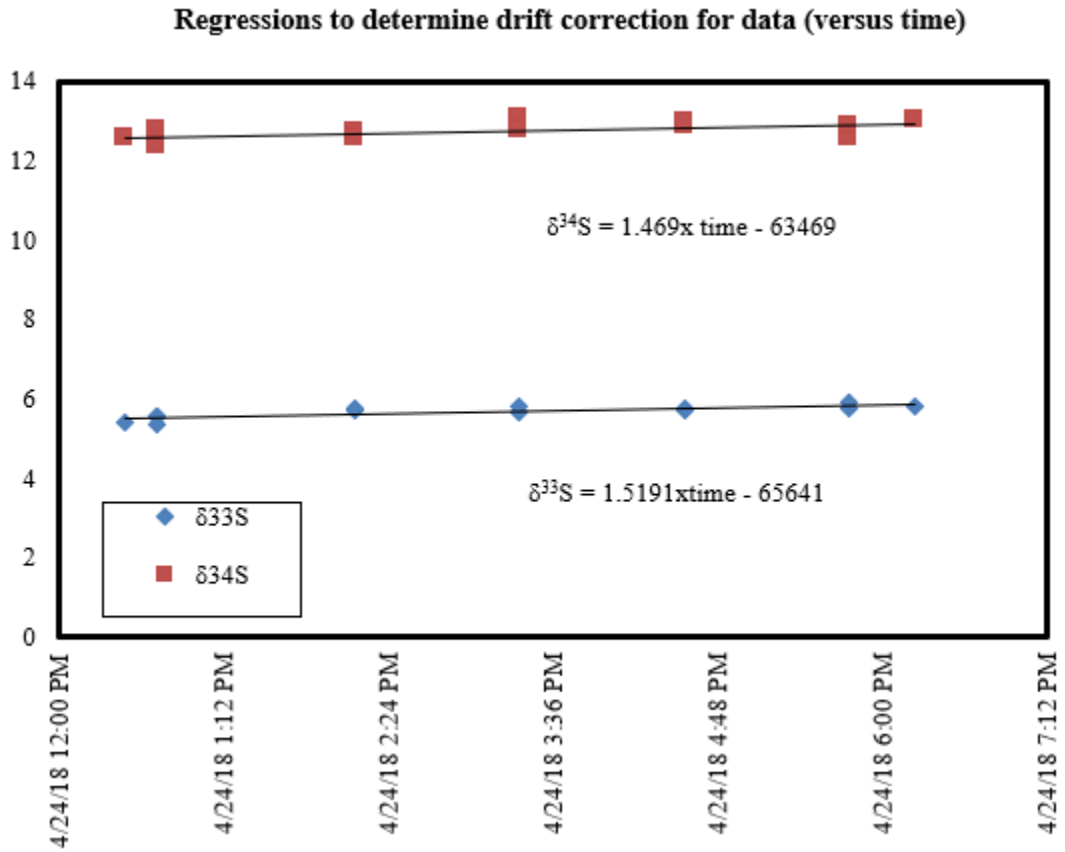

Table A3 Drift Corrected Data Normalized to CDT

Experiment	Species	$\delta^{33}S$	$\delta^{34}S$	$\Delta^{33}S$
1	initial sulfate	15.7	2.8	14.2
2	initial sulfate	15.8	2.9	14.3
3	Initial sulfate	16.4	2.9	14.9
1A	Elemental S	4.1	7.1	0.5
1B	Elemental S	4.0	7.0	0.4
1C	Elemental S	3.6	6.0	0.5
1A	Sulfate	15.7	3.4	14.0
1B	Sulfate	15.9	3.0	14.4
1C	Sulfate	15.4	3.4	13.7
2A	AVS	5.2	9.4	0.3
2B	AVS	5.2	9.4	0.4
2C	AVS	4.9	8.5	0.5
2A	Elemental S	5.3	9.3	0.6
2B	Elemental S	5.3	9.1	0.6
2C	Elemental S	5.1	9.0	0.5
2A	Sulfate	15.6	7.3	11.9
2B	Sulfate	17.9	10.8	12.4
2C	Sulfate	17.8	8.6	13.3
3A	AVS	2.1	-22.0	13.5
3B	AVS	2.5	-15.4	10.5
3C	AVS	**7.5**	**3.9**	**5.5**
3A	CRS	2.6	-19.9	12.9
3B	CRS	3.6	-13.0	10.3
3c	CRS	3.9	-15.4	11.9
3A	Sulfate	18.7	11.3	12.9
3B	Sulfate	17.4	14.6	9.9
3C	Sulfate	16.4	9.2	11.7
4A	AVS	3.0	-13.5	10.0
4B	AVS	2.6	-15.0	10.4
4C	AVS	1.6	-12.1	7.9
4A	CRS	4.0	-2.4	5.2
4A	CRS	3.2	-9.4	8.1
4B	CRS	3.3	-6.9	6.9
4B	CRS	3.4	-10.4	8.8
4B	CRS	3.5	-4.5	5.9
4C	CRS	3.1	-4.9	5.6
4A	Elemental S	4.6	4.8	2.2
4A	Elemental S	4.6	4.9	2.1
4B	Elemental S	5.1	8.5	0.7
4B	Elemental S	4.9	8.3	0.6
4C	Elemental S	4.6	4.5	2.3

4C	Elemental S	4.5	4.3	2.3
4A	Sulfate	17.0	10.6	11.5
4B	Sulfate	17.0	12.0	10.9
4C	Sulfate	22.4	20.6	11.8
NBS 127	Reference	10.8	21.1	0.0
NBS 127	Reference	10.9	21.3	0.0
NBS 127	Reference	10.9	21.0	0.1
NBS 127	Reference	10.7	20.8	0.0
NBS 127	Reference	11.0	21.1	0.1
NBS 127	Reference	11.0	21.0	0.2
NBS 127	Reference	11.0	21.4	0.0
NBS 127	Reference	10.8	21.1	0.0
NBS 127	Reference	10.8	21.1	0.0
NBS 127	Reference	10.8	21.2	-0.1
NBS 127	Reference	10.8	20.8	0.1
NBS 127	Reference	10.9	21.1	0.1
NBS 127	Reference	10.8	21.2	0.0

References

Berner, R. A. “Sedimentary pyrite formation.” American Journal of Science, vol. 268, no. 1, Jan. 1970, pp. 1–23.

Bowles, M. W., Mogollón, J. M., Kasten, S., Zabel, M., & Hinrichs, K. (2014). Global rates of marine sulfate reduction and implications for sub-sea-floor metabolic activities. Science, 344 (6186), 889-891.

Brysch, K., Schneider, C., Fuchs, G., & Widdel, F. (1987). Lithoautotrophic growth of sulfate-reducing bacteria, and description of *Desulfobacterium autotrophicum* gen. Archives of Microbiology, 148 (4), 264-274.

Cline, J. D. (1969). Spectrophotometric Determination of Hydrogen Sulfide in Natural Waters1. Limnology and Oceanography, 14 (3), 454-458.

Farquhar, J., Bao, H., & Thiemens, M. (2000). Atmospheric Influence of Earth's Earliest Sulfur Cycle. Science, 289 (5480), 756-758.

Farquhar, J., Peters, M., Johnston, D. T., Strauss, H., Masterson, A., Wiechert, U., & Kaufman, A. J. (2007). Isotopic evidence for Mesoarchaean anoxia and changing atmospheric sulphur chemistry. Nature, 449(7163).

Farquhar, J., Wing, Boswell A. (2003). Multiple sulfur isotopes and the evolution of the atmosphere. Desalination, 213 (1-2), 1-13.

Farquhar, J., J. Savarino, S. Airieau, and M. H. Thiemens (2001), Observation of wavelength-sensitive mass-independent sulfur isotope effects during SO2 photolysis: Implications for the early atmosphere, J. Geophys. Res., 106(E12), 32829–32839.

Farquhar, J., Cliff, J., Zerkle, A. L., Kamyshny, A., Poulton, S. W., Claire, M., & ... Harms, B. (2013). Pathways for Neoarchean pyrite formation constrained by mass-independent sulfur isotopes. Proceedings of The National Academy of Sciences of the United States of America, 110 (44), 17638-17643.

Halevy, I., & Bachan, A. (2017). The geologic history of seawater pH. Science, 355(6329), 1069-1071.

Kasting, James F. (1993). Earth's Early Atmosphere. Science, 259(5097), 920-926.

Luther, George III. (1991). Pyrite synthesis via polysulfide compounds Geochimica et Cosmochimica Acta 55(10):2839.

Navarrete, C. S., Zamorano, A., Ferrada, C., & Rodríguez, L. (2010). Sulphate reduction and biomass growth rates for *Desulfobacterium autotrophicum* in yeast extract – Supplemented media at 38°C. Desalination, 248 (1-3), 377-383.

Ohmoto, H. (1992). Biogeochemistry of sulfur and the mechanisms of sulfide–sulfate mineralization in Archean oceans. In: Schidlowski, M., et al. (Eds), Early Organic Evolution: Implications for Mineral and Energy Resources. Springer, Berlin, pp. 378-397.

Ono, Shuhei, et al. "Lithofacies control on Multiple-Sulfur isotope records and Neoarchean sulfur cycles." Precambrian Research, vol. 169, no. 1-4, 2009, pp. 58–67.

Ono, S., Eigenbrode, J., Pavlov, A., Kharecha, P., Rumble, D., Kasting, J., & Freeman, K. (2003). New insights into archean sulfur cycle from mass-independent sulfur isotope records from the hamersley basin, australia. Earth and Planetary Science Letters, 213(1-2), 15-30.

Rickard, D. (2014). The Sedimentary Sulfur System: Biogeochemistry and Evolution through Geologic Time. Treatise on Geochemistry, 267-326.

Roger Buick J. S. R. Dunlop. "Evaporitic Sediments of Early Archaean Age from the Warrawoona Group, North Pole, Western Australia." *Sedimentology*, vol. 37, no. 2, 1990, pp. 247–247.

Shen, Y., Farquhar, J., Masterson, A., Kaufman, A.J. and Buick, R., (2009). Evaluating the role of microbial sulfate reduction in the early Archean using quadruple isotope systematics. Earth and Planetary Science Letters, 279(3), pp.383-391.

Ueno, Y., Ono, S., Rumble, D., & Maruyama, S. (2008). Quadruple sulfur isotope analysis of ca. 3.5 Ga Dresser Formation: New evidence for microbial sulfate reduction in the early Archean. *Geochimica et Cosmochimica Acta*, *72*(23), 5675-5691.

Zhelezinskaia, I., Kaufman, A. J., Farquhar, J., & Cliff, J. (2014). Large sulfur isotope fractionations associated with Neoarchean microbial sulfate reduction. *Science*, *346*(6210), 742-744.

Honor Code

"I pledge on my honor that I have not given or received any unauthorized assistance or plagiarized."